Published online August 9, 2006

Transport of Coliphage in the Presence and Absence of Manure Suspension

Scott A. Bradford,* Yadata F. Tadassa, and Yan Jin

ABSTRACT

Mechanisms of coliphage transport and fate in the presence and absence of manure suspension were studied in saturated column experiments. In the presence of manure suspension, little inactivation of indigenous somatic coliphage occurred and the transport was controlled by deposition. The deposition followed a power law distribution with depth, and the magnitude increased with decreasing sand size. Comparison of the cumulative size distribution of manure components in the suspension initially and after passage through sand, suggested that particles retained by mechanical filtration and/or straining decreased the effective pore size and potentially induced straining of the somatic coliphage. A 2-site kinetic deposition model was used to estimate the magnitudes of attachment and straining in the presence of manure suspension, and provided a good description of the data. Modeling results indicated that straining accounted for 16 to 42% of the deposited somatic coliphage, and that both straining and attachment increased with decreasing sand size due to smaller pores and higher surface area, respectively. In the absence of manure suspension, ϕX174 (a representative somatic coliphage) and MS2 (a male-specific RNA coliphage) transport was controlled by inactivation induced by the solid phase. This conclusion was based on comparison of coliphage transport behavior at 5 and 20°C, mass balance information, and numerical modeling. Comparison of somatic coliphage transport data in the presence and absence of manure suspension revealed much higher effluent concentrations in the presence of manure. This difference was attributed to lower inactivation and higher detachment rates. The observed coliphage transport behavior suggests that survival of viruses may be extended in the presence of manure suspensions, and that transport studies conducted in the absence of manure suspension may not accurately characterize the transport potential of viruses in manure-contaminated environments.

Groundwater contamination by pathogenic viruses is common in many areas of the U.S.A. (Abbaszadegan et al., 2003). Most waterborne viruses are of fecal origin. An important agricultural source of fecal-contaminated water is wash water and storm water runoff from concentrated animal feeding operations (CAFOs). These CAFOs produce large quantities of manure, wash water, and storm water runoff. For example, over 272 million tons of manure were produced by confined beef and dairy cows in the U.S.A. in 1997 (Kellogg et al., 2000). Animal wastes contain a variety of viruses that are important pathogens to their animal hosts. The significance of these animal viruses to human health is uncertain, although some are known to be zoonotic (Reynolds, 2001).

S.A. Bradford and Y.F. Tadassa, USDA-ARS, George E. Brown, Jr., Salinity Laboratory, 450 W. Big Springs Road, Riverside CA 92507-4617. Y. Jin, Department of Plant and Soil Sciences, University of Delaware, Newark, DE 19716. Received 25 Jan. 2006. *Corresponding author (sbradford@ussl.ars.usda.gov).

Published in J. Environ. Qual. 35:1692–1701 (2006).
Technical Reports: Ground Water Quality
doi:10.2134/jeq2006.0036

677 S. Segoe Rd., Madison, WI 53711 USA

Dissemination of animal viruses in the environment occurs as a result of application of animal manure and contaminated water to agricultural lands, and partitioning of manure components to flowing water. Viruses in turn can be transported with water and manure suspensions to surface water and through soils to groundwater. Knowledge of the processes that control the transport and fate of animal viruses is therefore needed to assess the risk and vulnerability of water resources to contamination, and to develop cost-effective treatment strategies to minimize human and animal exposure.

Considerable research has been devoted to the fate and transport of viruses in porous media (Schijven and Hassanizadeh, 2000; Jin and Flury, 2002). Attachment, detachment, and inactivation mechanisms have been identified as key processes that control the fate of viruses in the environment. Attachment and detachment depend on virus-virus, virus-solvent and virus-porous media interactions (Elimelech and O'Melia, 1990). Although viruses can have variably charged surfaces due to the presence of ionizable amino acids in their protein capsid (Gerba, 1984), most possess a net negative charge at a neutral pH (Jin and Flury, 2002). Under these circumstances, virus deposition is believed to be controlled by attachment onto positively charged clay edges and metal (iron, aluminum, and manganese) oxide surfaces (Farrah and Preston, 1993; Jin et al., 1997; Lukasik et al., 1999; Zhuang and Jin, 2003a). The presence of metal oxides has also been reported to enhance virus inactivation (Sagripanti et al., 1993; Pieper et al., 1997; Schijven et al., 1999; Chu et al., 2001; Ryan et al., 2002).

Several researchers have examined the influence of organic matter on virus transport (Powelson et al., 1991; Pieper et al., 1997; Zhuang and Jin, 2003b; Foppen et al., 2006). In these studies, humic or fulic acids were commonly used as surrogates for sewage or manure effluent. Some researchers reported that dissolved organic matter (DOM) enhanced microbe transport (Pieper et al., 1997; Johnson and Logan, 1996; Powelson and Mills, 2001). Blocking of favorable attachment sites by organic matter has typically been used to explain this enhanced transport (Pieper et al., 1997; Johnson and Logan, 1996; Zhuang and Jin, 2003b; Foppen et al., 2006). DOM has also been reported to sorb onto microbes and alter their electrophoretic mobility (Gerritson and Bradley, 1987). Increasing the negative charge of microbe surfaces diminishes its attachment onto negatively charged solid surfaces (Sharma et al., 1985). Conversely, other researchers have reported that organic matter inhibits virus transport due to hydrophobic interactions between the virus and grain surfaces that are coated with organic matter (Bales et al., 1993; Kinoshita et al., 1993).

Manure suspensions consist of a complex mixture of partially digested organic matter and microbial bio-

mass, and therefore encompasses a wide range in particle sizes. Viruses represent only a small mass fraction of the total particles in suspensions. Straining of larger manure particles in down-gradient pores that are too small to allow particle passage would decrease the effective size of the pores or fill the smaller pore spaces completely. The potential implications of this manure deposition on virus transport are not yet known. Deposition-induced changes in the soil pore sizes could promote virus retention via straining, or induce changes in the pore-scale water flow field that would confine viruses to more conductive (larger and less reactive) regions of the pore space. Alternatively, adsorption of viruses onto mobile manure colloids could also potentially facilitate their transport potential (Jin et al., 2000; de Jonge et al., 2004).

This study examines the transport of indigenous somatic coliphage in dairy calf manure suspension and two indicator viruses (coliphage ϕX174 and MS2) in the absence of manure suspension. Special attention was given to mechanisms of virus attachment, detachment, straining, and inactivation. Effluent concentration curves and the final spatial distributions of the coliphage were measured in column transport studies, whereas inactivation behavior was quantified by comparing transport results at different temperatures. Data analysis and interpretation was aided through mathematical modeling, mass balance considerations, and measurement of the particle size distributions in the effluent.

MATERIALS AND METHODS

Coliphages MS2 and ϕX174 are commonly associated with fecal contamination and are typically found in high concentrations in lagoon water (Havelaar et al., 1986). Hence, MS2 and ϕX174 are recommended indicators for male-specific and somatic coliphage, respectively, in water and waste water (USEPA, 2001). Coliphage MS2 is an icosahedral single-stranded RNA phage with a diameter of 26.0 to 26.6 nm (Van Duin, 1988) and has an isoelectric point of 3.9 (Zerda, 1982). The electrostatic (zeta) potential of MS2 is -17.7 ± 2.3 mV in 0.01 *M* NaCl solution at a neutral pH (You et al., 2003). The surface of MS2 is negatively charged under most natural environmental pHs (Redman et al., 1997), has many similar physical properties to enteroviruses (Havelaar, 1993), and is a reasonable surrogate for enterovirus transport (Schijven and Hassanizadeh, 2000). The survival of MS2 was reported to be similar to that of human pathogenic viruses (Schijven and Hassanizadeh, 2000). Coliphage ϕX174 is a spherical, single-stranded DNA coliphage with a 27-nm diameter and an isoelectric point of 6.6 (Dowd et al., 1998). Considered to be a relatively conservative indicator for human virus transport, ϕX174 is environmentally stable and has low hydrophobicity (Schijven and Hassanizadeh, 2000).

Transport experiments were conducted using somatic coliphage that were indigenous to dairy calf manure suspension, MS2, and ϕX174. The concentrations of these coliphages in experimental solutions were determined by the soft-agar layer method (Adams, 1959). Approximately 2 mL of sample (influent, effluent, and soil solution) was collected for analysis. If the samples contained manure suspension, they were centrifuged at 10 000 rpm for 10 min (20°C). A serial dilution was made from 1 mL of the supernatant (manure suspension) or sample. One-half mL of log phase host bacterial strain was added to 3 mL of the soft trypticase soy agar (supplemented with nalidixic acid for indigenous somatic coliphage and ϕX174, and ampicillin and streptomycin for MS2) kept at 46°C with a water bath. The tube was immediately removed from the water bath and 100 μL of serial diluted solution was added. The content of the tube was gently mixed and poured onto the trypticase soy agar plate, swirled and allowed to solidify. The host bacterial strain for MS2 was *Escherichia coli* (ATCC #700891), whereas *E. coli* (ATCC #700609) was used as host for indigenous somatic coliphage and ϕX174. Plates were inverted and incubated at 37°C for 12 to 24 h. The number of plaque forming units (pfu) was then determined from plate counts.

Experimental solutions (deionized water) consisted of 0.001 *M* NaBr (influent suspension) or 0.001 *M* NaCl (resident and eluant solution) buffered to a pH of 6.73 using 5×10^{-5} *M* $NaHCO_3$. The electrical conductivity of this solution was 0.14 dS m^{-1}. In the absence of manure suspension, MS2 and ϕX174 were added to the 0.001 *M* NaBr (influent) solution at concentrations of 2×10^5 and 1.7×10^5 pfu mL^{-1}, respectively.

Unless specifically noted the transport experiments were conducted at approximately 20°C. To investigate coliphage transport under conditions of minimal inactivation, an additional experiment was run in a constant temperature cold room at 5°C. In this case, MS2 and ϕX174 were added to the 0.001 *M* NaBr (influent) solution at concentrations of 6.8×10^4 and 3.9×10^4 pfu mL^{-1}, respectively.

Holstein dairy calf manure was collected directly under the crates of 1- to 12-wk-old calves, thoroughly mixed with a stick, and stored at 4°C before use. The manure suspension was prepared by mixing a known mass of manure (wet weight) with the 0.001 *M* NaBr solution. This suspension was then filtered through a 103-μm stainless steel wire mesh. The concentrated suspension was then diluted to achieve a concentration of approximately 4.0 g l^{-1} (mass based on unfiltered weight). The pH and electrical conductivity of the filtered manure suspension were 8.8 and 0.38 dS m^{-1}, respectively. Particle size distribution information for the influent and selected effluent manure samples were determined using a Horiba LA 930 laser scattering particle size analyzer (Horiba Instruments, Irvine, CA 92614). The initial concentration of indigenous somatic coliphage in the manure suspension was approximately 1.2×10^4 pfu mL^{-1}, whereas no male-specific coliphage was detected.

Ottawa aquifer sand (U.S. Silica, Ottawa, IL) was used in the transport experiments. The Ottawa sands will be designated herein by the median grain size (d_{50}) as: 710, 360, 240, and 150 μm. The coefficient of uniformity ($U_i = d_{60}/d_{10}$; here x% of the sand was finer than d_x) of the 710, 360, 240, and 150 μm sands was 1.21, 1.88, 3.06, and 2.25, respectively. Pore size distribution information for these Ottawa sands can be calculated from the capillary pressure-saturation curve presented by Bradford and Abriola (2001). Ottawa sands typically consisted of 99.8% SiO_2 (quartz) and trace amounts of metal oxides, were spheroidal in shape, and had rough surfaces. The vast majority of the sands possessed a net negative charge at a neutral pH.

Many of the protocols for the column experiments were described in detail by Bradford et al. (2002); only a short summary is provided below. Borosilicate glass chromatography columns (Kimble/Kontes, Vineland, NJ) (15-cm long and 4.8 cm i.d.) equipped with a standard flangeless end fitting at the column bottom and an adjustable flow adaptor at the top were used in the experiments. The columns were wet-packed with the various porous media. The coliphage tracer suspension (with and without manure suspension) or eluant (0.001 *M* NaCl) solution was pumped upward through the vertically oriented columns at a steady rate for 250 min. Table 1 provides the porosity (ε), column length, the duration of the

Table 1. Soil column properties (manure suspension concentration, C_{im}, coliphage pulse duration, T_o, Darcy water velocity, q, porosity, ε; and column length, L_c) and the percent coliphage recovery in the effluent (M_{eff}), sand (M_{sand}), and the total system (M_{total}). The difference in M_{total} (ΔM_{total}) for somatic coliphage in the presence (indigenous) and absence (ϕX174) of the manure suspension is also provided.

Coliphage	d_{50}	C_{im}	T_o	q	ε	L_c	M_{eff}	M_{sand}	M_{total}	ΔM_{total}
	μm	mg L^{-1}	min	cm min^{-1}		cm				
MS2	710	0	75	0.10	0.35	12.9	59.9	0.0	59.9	
MS2	360	0	75	0.09	0.32	12.3	57.4	0.1	57.5	
MS2	240	0	75	0.09	0.34	12.6	38.9	0.2	39.1	
MS2	150	0	75	0.09	0.35	12.9	44.3	0.3	44.6	
MS2†	150	0	75	0.09	0.36	12.9	76.3	0.3	76.6	
ϕX174	710	0	75	0.10	0.35	12.9	48.8	0.1	48.9	
ϕX174	360	0	75	0.09	0.32	12.3	46.4	0.2	46.6	
ϕX174	240	0	75	0.09	0.34	12.6	67.1	0.1	67.2	
ϕX174	150	0	75	0.09	0.35	12.9	59.2	0.2	59.4	
ϕX174†	150	0	75	0.09	0.36	12.9	88.2	0.2	88.4	
Indigenous	710	4	75	0.12	0.36	12.0	93.7	2.0	95.7	46.8
Indigenous	360	4	75	0.10	0.33	12.5	91.8	4.0	95.8	49.2
Indigenous	240	4	75	0.11	0.33	12.4	94.2	4.7	98.9	31.7
Indigenous	150	4	75	0.09	0.35	12.8	76.9	9.6	86.5	27.1

† Experiments conducted at 5°C.

tracer suspension pulse, and the average aqueous Darcy velocity (q) for the various column experiments. Effluent samples were collected in glass test tubes over the course of each column experiment using an autosampler, and the concentration of coliphage was measured using the procedures outlined above.

Following completion of the transport experiments, the spatial distribution of reversibly retained coliphages in the sand was determined. The saturated sand was carefully excavated into 50 mL Falcon tubes containing excess 0.001 *M* NaBr solution. The tubes were then shaken for 15 min, and the concentration of coliphage in the excess solution was determined. The mass of water and sand in the tubes was determined by weight. A number balance was conducted at the end of each column experiment by normalizing the recovered coliphage number in the effluent and sand by the amount injected into the column.

Inactivation experiments were conducted in 20-mL glass scintillation vials filled with 20 mL of the coliphage suspension. Vials were capped and slowly mixed using a Labquake orbital shaker (Barnstead/Thermolyne, Dubuque, IA) for 250 min. Duplicate samples (100 μl) of excess suspension were periodically collected from the vials and analyzed for coliphage concentration.

The HYDRUS-1D computer code (Simunek et al., 1998; Bradford et al., 2003) was used to simulate coliphage transport and deposition in the column experiments. Aspects of HYDRUS-1D that are relevant to coliphage transport in the saturated column experiments are briefly discussed below. To minimize the number of fitted model parameters, the values of the hydrodynamic dispersivity (λ) that were used in the simulations were taken from bromide tracer data presented by Bradford et al. (2002) for the same sands and a similar velocity.

The aqueous phase coliphage mass balance equation is written as:

$$\frac{\partial(\theta_w C)}{\partial t} = -\nabla \cdot J_T - E_{sw} - \mu_w C \qquad [1]$$

where C [N_c L^{-3}; L denotes length and N_c is the number of coliphage] is the coliphage concentration in the aqueous phase, t [T] is time, θ_w [-] is the volumetric water content, J_T [N_c L^{-2} T^{-1}] is the total coliphage flux (sum of the advective, dispersive, and diffusive fluxes), μ_w [T^{-1}] is the coliphage inactivation rate in the aqueous phase, and E_{sw} [N_c L^{-3} T^{-1}] is the coliphage mass transfer terms between the aqueous and solid phases.

Two model formulations for E_{sw} will be considered in this work. The most complex 2-site kinetic model is written as:

$$E_{sw} = \frac{\partial[\rho_b(S_{att} + S_{str})]}{\partial t} = \theta_w k_{att} C - \rho_b k_{det} S_{att} + \theta_w k_{str} \psi_{str} C - \rho_b \mu_s (S_{att} + S_{str}) \qquad [2]$$

Here ρ_b [M L^{-3}; M denotes mass] is the soil bulk density, S_{att} [N_c M^{-1}] is the solid phase concentration of attached coliphage, S_{str} [N_c m^{-1}] is the solid phase concentration of strained coliphage, k_{att} [T^{-1}] is the attachment coefficient, k_{det} [T^{-1}] is the detachment coefficient, k_{str} [T^{-1}] is the straining coefficient, ψ_{str} [-] is a dimensionless straining function, and μ_s [T^{-1}] is the coliphage inactivation rate on the solid phase. Coliphage attachment, detachment, straining, and solid phase inactivation are modeled using the first, second, third, and fourth terms on the right hand side of Eq. [2], respectively.

The value of ψ_{str} in Eq. [2] is modeled as a function of distance and S_{str} as:

$$\psi_{str} = \left(1 - \frac{S_{str}}{S_{str}^{max}}\right)\left(\frac{d_{50} + z}{d_{50}}\right)^{-\beta} \qquad [3]$$

where z [L] is depth from the column inlet, S_{str}^{max} [N_c M^{-1}] is the maximum solid phase concentration of strained coliphage, and β [-] is a parameter that controls the shape of the (power law) spatial distribution. The first term on the right hand side of Eq. [3] accounts for filling and accessibility of straining sites in a manner similar to the Langmuirian blocking approach (Deshpande and Shonnard, 1999). The remaining term on the right-hand side of Eq. [3] assumes that coliphage deposition by straining occurs primarily at the column inlet, because the flow field is not yet fully established and coliphage therefore have increased accessibility to small pore spaces. The apparent number of small dead-end pores is hypothesized to decrease with increasing distance because size exclusion, advection, and transverse dispersivity tend to keep mobile coliphage within the larger networks, thus bypassing smaller pores.

For simplicity, an alternative 1-site kinetic formation for E_{sw} is also considered as:

$$E_{sw} = \frac{\partial(\rho_b S)}{\partial t} = \theta_w k_1 \psi_1 C - \rho_b k_{det} S - \rho_b \mu_s S \qquad [4]$$

Here S [N_c m^{-1}] is the solid phase concentration of coliphage, k_1 [T^{-1}] is the deposition coefficient, and ψ_1 [-] is a dimen-

sionless deposition function. In contrast to Eq. [2], deposition processes are lumped together in effective parameters in Eq. [4] and no attempt is made to separate attachment and straining mechanisms. To have the most flexibility to describe spatial distribution data, the value of ψ_1 in Eq. [4] is modeled in an analogous manner to Eq. [3]. In this case, however, ψ_1 is viewed as an empirical parameter that characterizes the observed spatial distribution and a physical interpretation for this distribution is not implicitly assumed.

RESULTS AND DISCUSSION

Coliphage Transport in the Presence of Manure Suspension

Indigenous somatic coliphage was found in the manure suspension at an initial concentration (C_i- N_c L^{-3}) of approximately 1.2×10^4 pfu mL^{-1}, whereas male-specific coliphage was not detected. Somatic coliphage commonly persist longer than male-specific coliphage (Schijven and Hassanizadeh, 2000). Transport experiments in the presence of manure suspension therefore only considered indigenous somatic coliphage. Figures 1a and 1b present effluent concentration curves and spatial distribution data for indigenous somatic coliphage in the manure suspension, respectively, in 710, 360, 240, and 150 μm sands. The relative effluent concentrations (C/C_i) were plotted as a function of pore volumes (PV) in Fig. 1a. In Fig. 1b the normalized concentration (number of coliphage, N_c, divided by the total number added to the column, N_{tc}) per gram of dry sand was plotted as a function of dimensionless depth (distance divided by the column length) from the column inlet. Percent recovery for somatic coliphage in the effluent (M_{eff}), sand (M_{sand}), and the total system (M_{total}) are provided in Table 1. Total amounts recovered were quite high (86.5 to 95.8%), indicating a high degree of confidence in both effluent and spatial distribution data and low amounts of inactivation and/or irreversible sorption. Effluent concentrations for the 710, 360, and 240 μm sand were of a similar magnitude (M_{eff} ranged from 91.8 to 94.2%), whereas somatic coliphage concentrations in the finest 150 μm sand were somewhat lower (M_{eff} = 76.9%) due to greater deposition (Table 1).

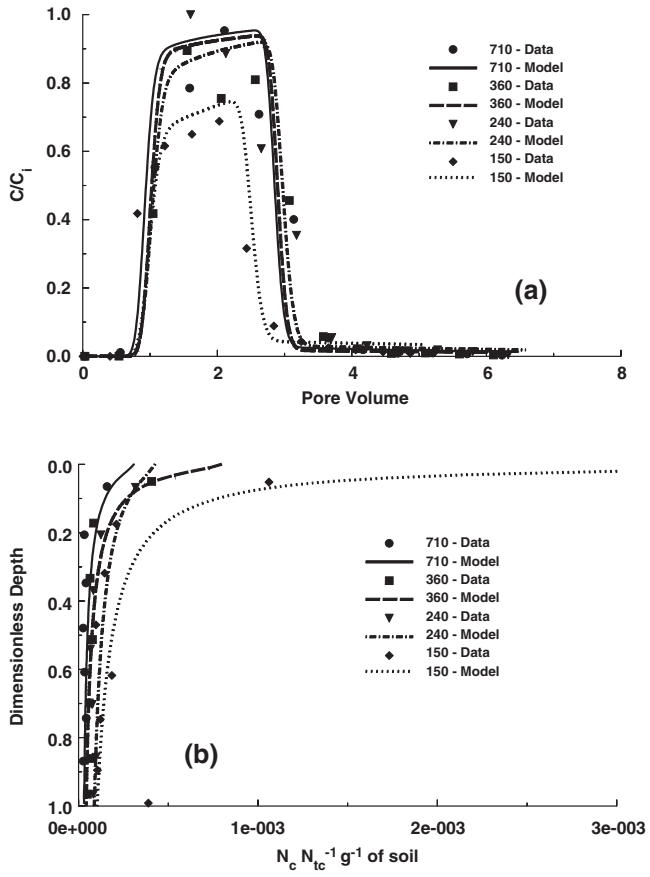

Fig. 1. Observed and simulated effluent concentration curves (Fig. 1a) and spatial distributions (Fig. 1b) for indigenous somatic coliphage in manure suspension in 710-, 360-, 240-, and 150-μm sand. Simulations considered 1-site kinetic deposition (Eq. [1], [3] and [4]) and corresponding model parameters are given in Table 2.

Spatial distribution data shown in Fig. 1b indicates two distinct deposition zones. In the first region (dimensionless depth < 0.2) somatic coliphage concentrations tended to be highest near the column inlet and then rapidly decreased with increasing distance. In the second region (dimensionless depth of 0.2 to 1.0) the distribution of somatic coliphage was more uniform with increasing depth. In both regions, somatic coliphage concentrations tended to increase with decreasing sand size.

Interpretation of effluent and spatial distribution data of the somatic coliphage was facilitated by considering the fate of other manure components in the suspension. Figure 2 presents the cumulative size distribution of manure particles in the suspension initially and after 95 min (around 2.2 pore volumes) of passage through the various sands. More comprehensive information on manure suspension transport and deposition in these same sands was recently presented by Bradford et al. (2006). The initial manure suspension encompasses a wide range of particle sizes (<103 μm). Manure particles larger than around 13, 2, 1, and 1 μm were completely removed after passage through the 710, 360, 240, and 150 μm sands, respectively, due to mechanical filtration. This corresponded to ratios of manure particle to median grain size of 0.4 to 1.8%. Since the sands encompassed a wide range of pore sizes, it is logical to anticipate that straining and/or mechanical filtration processes can also play an important role in the deposition of smaller particles. Furthermore, particles retained by straining and/or mechanical filtration can decrease the effective pore size. Deposition of particles smaller than 5.4 μm could therefore induce straining of 27 nm coliphage (ϕX174) according to the criterium ($27 \times 100/5400 = 0.5\%$) proposed by Bradford et al. (2003).

Mechanical filtration produces deposition primarily at the soil surface (McDowell–Boyer et al., 1986). Recent research by Bradford et al. (2002, 2003, 2004) and Bradford and Bettahar (2005) have similarly demonstrated that deposition of strained colloids (0.45 to 3.2 μm carboxyl latex and *Cryptosporidium* oocysts) occurred primarily at the sand surface. Hence, the coliphage spatial distributions (dimensionless depth < 0.2) shown in Fig. 1b were consistent with straining near the column inlet. Since straining increases with decreasing sand size,

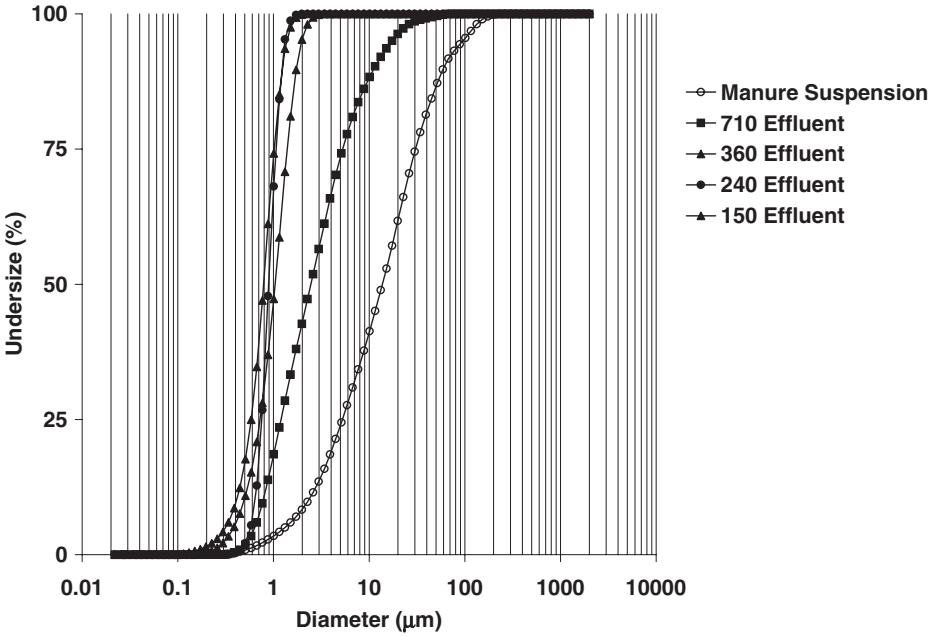

Fig. 2. The cumulative size distribution for manure particles before and after passage through 710-, 360-, 240-, and 150-μm sand.

the peak effluent concentration in the 150 μm sand was also lower than in the coarser textured sands (Fig. 1a). Straining of somatic coliphage could have been caused by decreases in the pore size that were induced by manure deposition or by direct association of the coliphage with larger manure particles. To test the latter hypothesis, the concentration of coliphage in the manure suspension was determined before and after centrifugation. The concentrations were nearly identical before and after centrifugation (within the uncertainty of replicate measurements), suggesting minimal attachment of the coliphage onto larger manure particles. For dimensionless depths of 0.2 to 1.0, coliphage deposition was believed to be controlled by attachment. In this region, higher concentrations of somatic coliphage occurred at a particular location for decreasing sand grain size, suggesting that the higher surface area sands produced greater attachment.

Figures 1a and 1b also present simulated somatic coliphage transport data using the 1-site kinetic deposition model. In this case, both attachment and straining processes were lumped together and no attempt was made to separate the mechanisms. Water and solid phase inactivation rate coefficients were assumed to be zero, because the recovered amounts of coliphage were quite high (86.5 to 95.8%). To improve the description of the spatial distribution, values of k_1, β, and S^{*max} (= S^{max}/N_{ic}; where $N_{ic} = C_i \times 1$ mL) were initially fitted to only the deposition data. These fitted values served as initial estimates in the simulations that also included effluent data. In this case, values of k_1 and k_{det} were fitted to the effluent data. Table 2 provides a summary of model parameters (k_1, β, S^{*max}, k_{det}, and λ), as well as statistical parameters (coefficient of linear regression to effluent, r_e^2, and spatial distribution data, r_s^2) to characterize the goodness of parameter fits. The simulated behavior shown in Fig. 1a and 1b and statistical parameters in Table 2 indicates that this model provided a reasonable description of both effluent and spatial distribution data.

To better deduce mechanisms of somatic coliphage deposition, the transport data was also simulated using the 2-site kinetic model. To separate the magnitudes of straining and attachment the spatial distribution data was divided into two regions. The first region (dimensionless depths of approximately 0 to 0.5) was initially characterized using fitted 1-site kinetic model parameters (k_1, β, and S^{*max}). The remaining portion of the spatial distribution was then characterized by fitting a value of k_{att} (irreversible attachment). With values of k_{att} determined by this procedure, new values of k_{str}, β, and S^{*max}_{str} were then fitted to the complete spatial distribution data. To include the influence of detachment,

Table 2. One-site kinetic deposition model (Eq. [1], [3], and [4]) parameters for indigenous somatic coliphage in the manure suspension. Here λ_H comes from Bradford et al. (2002), and the values of k_1, k_{det}, S^{*max}, and β were fitted to the transport data.

d_{50}	λ_H	k_1	k_{det}	S^{*max}	β	r_e^2	r_s^2
μm	cm	h^{-1}	h^{-1}	$N_c\,N_{ic}^{-1}\,g^{-1}$			
710	0.080	5.88	0.335	0.139	0.905	0.89	0.85
360	0.070	10.62	0.182	0.196	0.929	0.90	0.92
240	0.094	12.54	0.226	0.120	0.739	0.90	0.85
150	0.104	36.12	0.150	6.588	0.880	0.81	0.84

Table 3. Two-site kinetic deposition model (Eq. [1], [2], and [3]) parameters for indigenous somatic coliphage in the manure suspension. Here λ_H comes from Bradford et al. (2002), k_{det} comes from Table 2, and k_{att}, k_{str}, S^{*max}_{str}, and β were fitted to the transport data.

d_{50}	λ_H	k_{att}	k_{det}	k_{str}	S^{*max}	β	r_e^2	r_s^2
μm	cm	h^{-1}	h^{-1}	h^{-1}	$N_c\,N_{ic}^{-1}\,g^{-1}$			
710	0.080	0.234	0.335	4.32	0.042	1.362	0.89	0.96
360	0.070	0.221	0.182	2.52	0.095	0.743	0.89	0.89
240	0.094	0.280	0.226	5.58	0.368	0.996	0.90	0.97
150	0.104	0.254	0.150	25.86	0.912	1.167	0.82	0.87

the value of k_{att} was increased by a factor equal to k_{det} (Table 2). Table 3 provides a summary of model parameters (k_{str}, β, S_{str}^{*max}, k_{att}, k_{det}, and λ), and statistical parameters for the goodness of model fit. The 2-site model simulations were very comparable to the 1-site modeling results presented in Fig. 1a and 1b, and were therefore not shown. The estimated percentage of somatic coliphage deposition due to straining for the 710, 360, 240, and 150 μm sand was 16, 38, 32, and 42%, respectively. Values of k_{att} minus k_{det} (Table 3) increased with decreasing sand size, suggesting that attachment increased with increasing surface area of the sand.

Coliphage Transport in the Absence of Manure Suspension

Figures 3a and 3b present effluent concentration curves for MS2 and ϕX174, respectively, in 710-, 360-, 240-, and 150-μm Ottawa sands. The percentage of coliphage recovered in the effluent (M_{eff}) is given in Table 1. Decreasing the sand size tended to produce lower effluent concentrations for MS2 (M_{eff} ranged from 59.9 to 38.9%). The sand gradation may have also played a role in transport, since the more graded 240-μm sand exhibited slightly lower effluent concentrations (M_{eff} = 38.9%) than the 150-μm sand (M_{eff} = 44.3%). In contrast, ϕX174 exhibited the opposite trend with respect to sand size and gradation than MS2 (M_{eff} ranged from 46.6 to 67.2%).

After completion of the effluent transport portion of the experiment, the sands were excavated from the columns and the spatial distributions of reversibly retained coliphage were determined. Figures 4a and 4b present MS2 and ϕX174 spatial distribution data in the various sands, respectively. The spatial distributions were highly dependent on the coliphage type and the sand size. In Fig. 4a most of the MS2 deposition occurred at the column inlet, with increasing retention occurring with decreasing sand size. In contrast, ϕX174 exhibited more uniform deposition with depth.

The recovered percentages of coliphage in the sands (M_{sand}) were presented in Table 1. Very low values of M_{sand} (0.0 to 0.3%) were recovered for MS2 and ϕX174. The total amounts of coliphage ($M_{total} = M_{sand} + M_{eff}$) that were recovered were also quite low, suggesting that the remaining coliphage was either irreversibly sorbed to the sands or inactivated. Losses in the column setup were quantified by running a blank column experiment (similar flow rate and volume) without any sand. Influent and final effluent concentrations after 250 min were very similar, suggesting that minimal coliphage losses were attributable to the experimental setup.

To better understand mechanisms of solid inactivation and/or irreversible sorption, additional column experi-

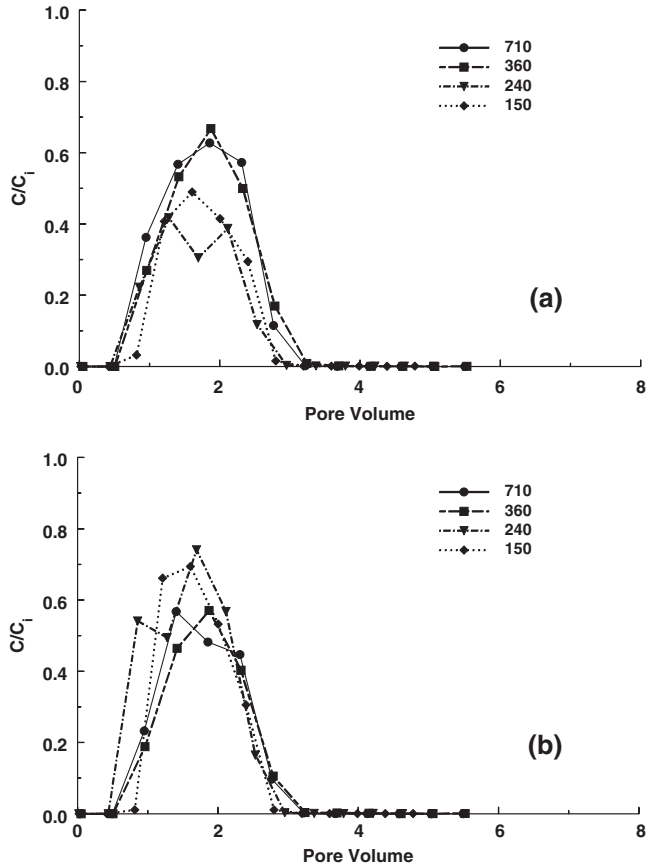

Fig. 3. Effluent concentration curves for MS2 (Fig. 3a) and ϕX174 (Fig. 3b) in 710-, 360-, 240-, and 150-μm sand in the absence of manure suspension.

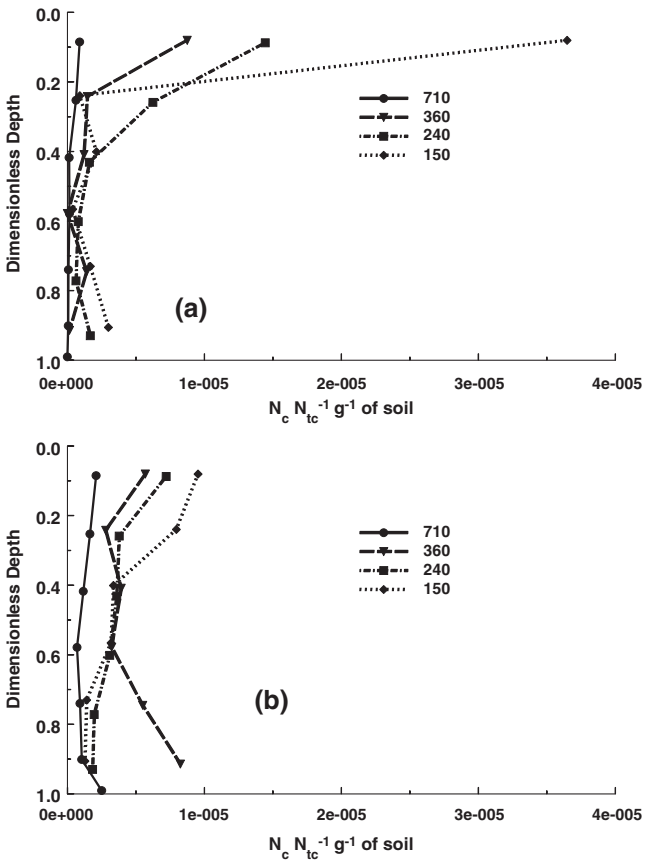

Fig. 4. Spatial distribution data for deposited MS2 (Fig. 4a) and ϕX174 (Fig. 4b) in 710-, 360-, 240-, and 150-μm sand in the absence of manure suspension.

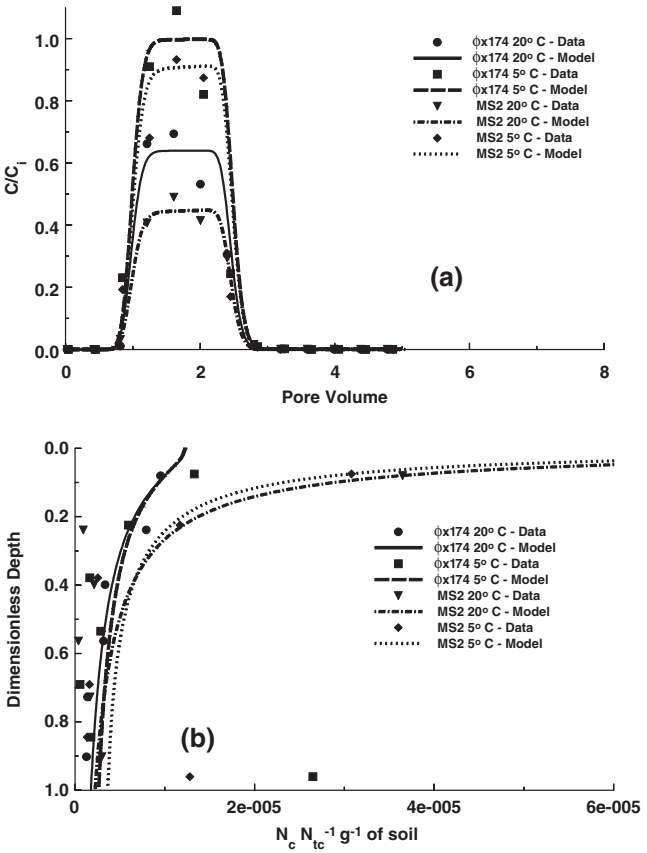

Fig. 5. Observed and simulated effluent concentration curves (Fig. 5a) and spatial distributions (Fig. 5b) for ϕX174 and MS2 in 150-μm sand in the absence of manure suspension and at 5 and 20°C. Here simulations considered 1-site kinetic deposition according to Eq. [1], [3], and [4]. Model parameters are provided in Table 4.

ments were conducted for ϕX174 and MS2 in 150-μm sand at an experimental temperature of 5°C. Significantly less inactivation was expected at 5 than 20°C (Schijven and Hassanizadeh, 2000; Jin and Flury, 2002). Figures 5a and 5b present effluent concentration curves (Fig. 5a) and spatial distribution data (Fig. 5b) for ϕX174 and MS2 in 150-μm sands at 5 and 20°C. Peak effluent concentration curves were much higher at 5 than at 20°C. Filtration theory predicts that the attachment coefficient will only slightly decrease (around 3.5% for a change in temperature from 20 to 5°C) with decreasing temperature (McCaulou et al., 1995). Hence, differences in transport behavior at 5 and 20°C were primarily due to inactivation. Comparison of M_{eff} values at 20°C (M_{eff} equaled 59% for ϕX174 and 44% for MS2) and 5°C (M_{eff} equaled 88% for ϕX174 and 76% for MS2) in this sand suggests that 29% of the ϕX174 and 32% of the MS2 were inactivated at 20°C in the 150-μm sands. The very low values of M_{sand} (0.2 to 0.3%) in both 5 and 20°C systems also suggests that solid phase inactivation was an important elimination process. The presence of trace amounts of metal oxides and/or metal ions on sand surfaces has been reported to control solid phase inactivation (Sagripanti et al., 1993; Pieper et al., 1997; Schijven et al., 1999; Chu et al., 2001; Ryan et al., 2002).

Figures 5a and 5b also present simulated effluent concentration curves (Fig. 5a) and spatial distributions (Fig. 5b) for ϕX174 and MS2 in 150-μm sands at 5 and 20°C. The 1-site kinetic model was used to describe this transport data, and no attempt was made to separately deduce mechanisms of attachment and straining because of the confounding influence of inactivation. At 5°C we assumed that water phase inactivation was negligible (consistent with batch inactivation results discussed below) and values of k_1, $k_{det,}$ S^{*max}, β and μ_s were determined from the transport data. At 20°C values of k_1, S^{*max}, β, and k_{det} were taken from the corresponding 5°C data (assuming that temperature had only a minor influence on deposition), and values of μ_s and μ_w were directly fitted to effluent and spatial distribution data, respectively. Table 4 summarizes the fitted model parameters, as well as statistical parameters for the goodness of the model fit to the data. The simulations provided a reasonable description of both effluent and spatial distribution data at 5 and 20°C.

Transport data for MS2 in the 710-, 360-, and 240-μm sands at 20°C were simulated using values of μ_s, μ_w, and k_{det} estimated from the 150-μm sand data, and by fitting values of k_1, S^{*max}, and β to the transport data. A similar approach was taken for the 20°C data for ϕX174 in these same sands, except a separate value of μ_w had to be fitted to the data from the 710- and 360-μm sands. Table 4 also summarizes these fitted model parameters. The values of r_e^2 and r_s^2 in Table 4 indicate that this approach generally provided a reasonable description of the transport data. Values of r_s^2 for ϕX174 data were sometimes low due to scatter in the measurement points.

The simulations discussed above provide insight on ϕX174 and MS2 inactivation in the various sands. Table 4 implies that changes in the sand size had a minimal impact on μ_s for a given coliphage. The dependence on sand size was presumably already accounted for by

Table 4. One-site kinetic deposition model (Eq. [1], [3], and [4]) parameters for MS2 and ϕX174 in the absence of manure suspension.

Coliphage	d_{50}	μ_w	μ_s	k_1	k_{det}	S^{*max}	β	r_e^2	r_s^2
	μm	h^{-1}	h^{-1}	h^{-1}	h^{-1}	$N_c N_{ic}^{-1}$ g^{-1}			
MS2	710	0.86	0.77	0.38	0.139	0.002	1.22	0.84	0.97
MS2	360	0.86	0.77	20.67	0.139	0.032	1.50	0.97	0.96
MS2	240	0.86	0.77	17.83	0.139	0.023	1.12	0.97	0.89
MS2	150	0.86	0.77	32.58	0.139	0.465	1.10	0.99	0.92
MS2†	150	0.00	0.88	32.58	0.139	0.465	1.10	0.91	0.83
ϕX174	710	0.94	0.01	0.07	0.107	0.000	0.74	0.98	0.03
ϕX174	360	1.00	0.01	0.32	0.107	0.001	0.46	0.97	0.86
ϕX174	240	0.53	0.01	0.13	0.107	0.002	0.67	0.69	0.96
ϕX174	150	0.53	0.01	0.55	0.107	0.002	0.83	0.96	0.90
ϕX174†	150	0.00	0.01	0.55	0.107	0.002	0.83	0.92	0.01

† Experiments conducted at 5°C.

the product of μ_s and S in Eq. [4], where S (deposition) implicitly included a dependence on the sand size. The value of μ_s in a given sand was much higher (77 to 88 times greater) for MS2 than ϕX174, indicative of an increased sensitivity to solid phase inactivation. Table 4 also indicates that similar values of μ_s occurred for a particular coliphage at 5 and 20°C in 150-μm sand. This observation suggests that solid phase inactivation can still be important even at 5°C.

The relative concentrations of ϕX174 and MS2 slowly decreased with increasing time in batch studies conducted at 20°C in the absence of sand. The value of μ_w was assumed to be first order and therefore determined as $\ln(C/C_i)/t_e$; where t_e is the equilibration time. The batch value of μ_w was measured to be 0.03 h^{-1} for MS2 and 0.01 h^{-1} for ϕX174. In general, ϕX174 is more stable (survives longer) than MS2 (DeBorde et al., 1998). Measured batch values of μ_w were much smaller (0.03 h^{-1} compared to 0.86 h^{-1} for MS2; and 0.01 h^{-1} compared to 0.53 to 1.00 h^{-1} for ϕX174) than those determined in the column studies (Table 4) and suggests that the solid phase impacted the measured value of μ_w in the column experiments. In further support of DeBorde's hypothesis, note in Table 4 that μ_w was similar in magnitude to μ_s for MS2 at 20°C. Schijven et al. (1999) also found that inactivation of deposited MS2 was similar to that of free MS2 in the water. In contrast, for ϕX174 the value of μ_w was 53 to 100 times greater than μ_s, with higher values of μ_w occurring in the coarser textured sands. Water phase ϕX174 was apparently more susceptible to inactivation than deposited ϕX174, especially in the coarser textured sands. We hypothesize that dissolution of metal ions into the aqueous phase may have influenced the water phase inactivation rates for ϕX174 (Sagripanti et al., 1993). The presence of different types of metals and surface oxide coatings in the various sands may have also contributed to differences in μ_w in the various sands.

Somatic Coliphage Transport in the Presence and Absence of Manure Suspension

The coliphage ϕX174 is a recommended indicator for somatic coliphage in water and waste water (USEPA, 2001). In this section we compare and contrast transport behavior of ϕX174 in the absence of manure suspension with indigenous somatic coliphage in manure suspension. Effluent and spatial distribution concentrations for the somatic coliphage were much higher in the presence (Fig. 1a and 1b) than in the absence of manure suspensions (Fig. 3b and 4b). For a given sand, the difference in M_{total} in the presence and absence of manure was 27.1 to 46.8% (Table 1), with greater differences occurring in coarser textured sands. Tables 2 and 4 indicate that the deposition coefficient was actually much higher in the presence of manure suspension than in the absence. Hence, all of these observations suggest that inactivation losses for somatic coliphage were much lower in the presence of manure suspension. This has important implications for virus fate in the field, and suggests that the viability of viruses may be enhanced in the presence of manure suspensions. Hence, transport studies conducted in the absence of manure suspension may not accurately characterize the transport potential of viruses in manure-contaminated environments.

The deposition coefficient (straining + attachment) was much higher in the presence of manure suspension than in the absence (Tables 2 and 4) due to differences in straining and attachment. Straining is expected to be much more significant in the presence of manure suspension than in the absence due to deposition of larger manure particles that can induce changes in the pore structure. Attachment may also be greater in the presence of manure suspension due to increases in the solution salinity (0.14 dS m^{-1} in the absence of manure suspension and 0.38 dS m^{-1} in the presence) (Zhuang and Jin, 2003b; Deshpande and Shonnard, 1999). Conversely, others researchers have postulated that attachment decreases in the presence of manure suspension due to blocking of favorable attachment sites (Pieper et al., 1997; Johnson and Logan, 1996; Powelson and Mills, 2001). We were unable to test this hypothesis due to the confounding influences of inactivation and straining.

After recovery of the bulk of the effluent concentration pulse, the coliphage breakthrough curves exhibited low concentration tailing (C/C_i values of around 10^{-3} to 10^{-4}). Figure 6 presents a semilog plot of observed and simulated somatic coliphage effluent concentration curves for 150-μm sand in the presence and absence of manure suspension. One-site kinetic deposition model parameters are provided in Tables 2 and 4. The observed tailing behavior shown in Fig. 6 is fairly accurately described using a first-order detachment term. After around 3 PV, both effluent concentration curves exhibited low concentration tailing behavior, slowly decreasing with continued flushing with 0.001 M NaCl solution as a result of detachment. The relative concentration of somatic coliphage in the manure suspension was around 2.5 orders of magnitude higher than in the absence. Similar concentration tailing behavior was observed for somatic coliphage in the other sands. Higher effluent concentrations in the presence of manure suspension were previously (when PV were <3) attributed to lower inactivation rates. In the tailing region (>3 PV), higher effluent concentrations may also be due to higher detachment rates of somatic coliphage from manure particles and/or manure-induced changes in the sand surface properties. In the absence of manure suspension, both MS2 and ϕX174 exhibited similar levels of low concentration tailing ($C/C_i = 10^{-3}$ to 10^{-4}) for the various sands.

CONCLUSIONS

Mechanisms of coliphage transport and fate in the presence and absence of dairy calf manure suspension were studied in saturated column experiments. In the presence of manure suspension, high recoveries of indigenous somatic coliphage in effluent and sand samples suggested that little inactivation occurred during the experiments, and that transport was controlled by deposition processes. In contrast to clean-bed filtration theory predictions, the spatial distribution of deposited

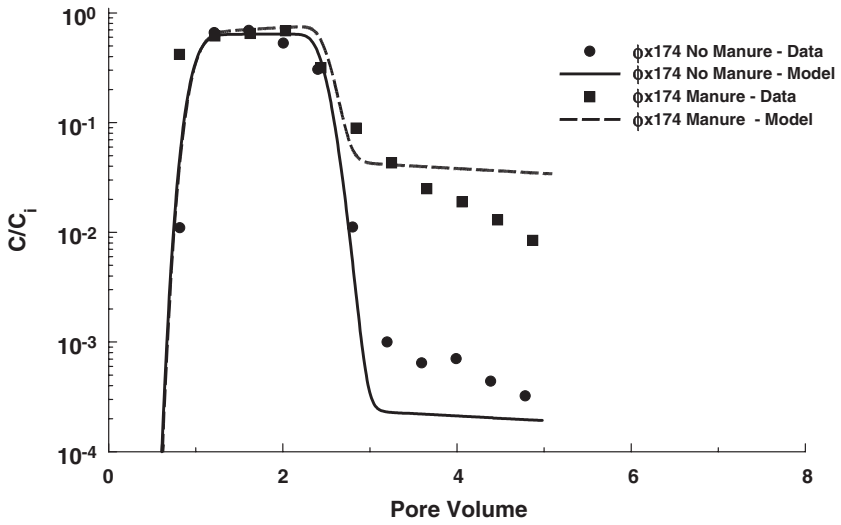

Fig. 6. A semilog plot of observed and simulated somatic coliphage effluent concentration curves in 150-μm sand in the presence (indigenous somatic coliphage) and absence (ϕX174) of manure suspension. One-site kinetic deposition model parameters are provided in Tables 2 and 4.

somatic coliphage was not exponential, but followed a power law distribution. Decreasing the sand size tended to produce increased deposition of somatic coliphage.

Interpretation of effluent and spatial distribution data for the somatic coliphage was facilitated by considering the fate of other manure components in the suspension. The cumulative size distribution of manure components in the suspension initially and after passage through the packed columns was measured, and used to identify the mechanical filtration potential of these sands. Manure particles were completely removed by mechanical filtration when d_p/d_{50} (d_p = manure particle diameter) was greater than 0.4 to 1.8%. This suggests that particles retained by straining and/or mechanical filtration can decrease the effective pore size, and may induce straining of much smaller particles such as coliphage. Comparison of somatic coliphage concentrations in the manure suspension before and after centrifugation suggested that the vast majority of the somatic coliphage was not attached to the manure particles.

A 2-site kinetic deposition model was used to estimate the magnitudes of somatic coliphage attachment and straining in the various sands in the presence of the manure suspension. The magnitude of attachment was estimated from the spatial distribution data in the region that exhibited relatively uniform deposition with depth (dimensionless depths 0.2 to 1). With fixed values of the attachment coefficient, the straining parameters were then fitted to the spatial distribution data. This modeling approach provided a good description for both effluent and spatial distribution data, and indicated that straining accounted for 16 to 42% of the deposited somatic coliphage in the various sands. Magnitudes of both straining and attachment increased with decreasing sand size due to smaller pores and higher surface area, respectively.

In the absence of manure suspension, the transport of ϕX174 and MS2 was controlled by solid and liquid phase inactivation. This conclusion was based on comparison of transport behavior for these coliphage at 5 and 20°C, mass balance information, and numerical modeling. At 5°C water phase inactivation was low and effluent concentration for ϕX174 and MS2 were high in the finest sand. In this case, deposition coefficients and solid phase inactivation rates were fitted to the transport data, and the numerical simulations provided a reasonable description of the observed data. Fitted values of the solid phase inactivation rate suggested that this process can still be important at 5°C (especially for MS2), presumably due to interactions with trace amounts of metal oxides and/or metals on sand grain surfaces. Effluent concentration for ϕX174 and MS2 in the finest sand at 20°C were much lower than at 5°C. Fitted values of the water phase inactivation rate were higher than those measured in the influent suspension, suggesting that the presence of the solid phase also influenced the water phase inactivation rate in these systems.

Comparison of somatic coliphage transport data in the presence (indigenous somatic coliphage) and absence (ϕX174) of manure suspension revealed much higher effluent concentrations in the presence of manure. This observation was attributed to differences in inactivation. In the presence of manure suspension, much lower inactivation occurred, presumably due to sorption of organic components onto metals and/or metal oxide surfaces that otherwise would have induced inactivation (Foppen et al., 2006). After recovery of the bulk of the breakthrough curve, low concentration tailing was observed for both indigenous somatic coliphage and ϕX174. In the presence of manure, the relative concentration for somatic coliphage in this tailing region was around 2.5 orders of magnitude higher in the presence than in the absence of manure. This may be due to lower inactivation rates and higher detachment rates in the presence of manure. The observed coliphage transport behavior has important implications for virus fate in the environment, and suggests that the viability of viruses may be enhanced in the presence of manure suspensions. Hence, transport studies conducted in the absence of manure suspension may not accurately characterize the transport potential of viruses in manure-contaminated environments.

ACKNOWLEDGMENTS

This research was supported by the 206 Manure and Byproduct Utilization Project of the USDA-ARS. Mention of trade names and company names in this manuscript does not imply any endorsement or preferential treatment by the USDA.

REFERENCES

Abbaszadegan, M., M.W. LeChevallier, and C.P. Gerba. 2003. Occurrence of viruses in US groundwaters. J. Am. Water Works Assoc. 95(9):107–120.

Adams, M.H. 1959. *Bacteriophages.* Interscience Publishers, NY, USA.

Bales, R.C., S. Li, K.M. Maguire, M.T. Yahya, and C.P. Gerba. 1993. MS-2 and poliovirus transport in porous media: Hydrophobic effects and chemical perturbations. Water Resour. Res. 29:957–963.

Bradford, S.A., and L.M. Abriola. 2001. Dissolution of residual tetrachloroethylene in fractional wettability porous media: Incorporation of interfacial area estimates. Water Resour. Res. 37:1183–1195.

Bradford, S.A., S.R. Yates, M. Bettahar, and J. Simunek. 2002. Physical factors affecting the transport and fate of colloids in saturated porous media. Water Resour. Res. 38(12): Art no. 1327, doi:10.1029/2002WR001340.

Bradford, S.A., J. Simunek, M. Bettahar, M.Th. van Genuchten, and S.R. Yates. 2003. Modeling colloid attachment, straining, and exclusion in saturated porous media. Environ. Sci. Technol. 37:2242–2250.

Bradford, S.A., M. Bettahar, J. Simunek, and M.Th. Van Genuchten. 2004. Straining and attachment of colloids in physically heterogeneous porous media. Vadose Zone J. 3:384–394.

Bradford, S.A., and M. Bettahar. 2005. Straining, attachment, and detachment, of Cryptosporidium oocysts in saturated porous media. J. Environ. Qual. 34:469–478.

Bradford, S.A., Y.F. Tadassa, and Y.A. Pachepsky. 2006. Transport of *Giardia* and manure suspensions in saturated porous media. J. Environ. Qual. 35:749–757.

Chu, Y., Y. Jin, M. Flury, and M.V. Yates. 2001. Mechanisms of virus removal during transport in unsaturated porous media. Water Resour. Res. 37:253–263.

DeBorde, D.C., W.W. Woessner, B. Lauerman, and P.N. Ball. 1998. Virus occurrence in a school septic system and unconfined aquifer. Ground Water 36:825–834.

de Jonge, L.W., C. Kjaergaard, and P. Moldrup. 2004. Colloids and colloid-facilitated transport of contaminants in soils: An introduction. Vadose Zone J. 3:321–325.

Deshpande, P.A., and D.R. Shonnard. 1999. Modeling the effects of systematic variation in ionic strength on the attachment kinetics of Pseudomonas fluorescens UPER-1 in saturated sand columns. Water Resour. Res. 35(5):1619–1627.

Dowd, S.E., S.D. Pillai, S.Y. Wang, and M.Y. Corapcioglu. 1998. Delineating the specific influence of virus isoelectric point and size on virus adsorption and transport through sandy soils. Appl. Environ. Microbiol. 64:405–410.

Elimelech, M., and C.R. O'Melia. 1990. Kinetics of deposition of colloidal particles in porous media. Environ. Sci. Technol. 24:1528–1536.

Farrah, S.R., and D.R. Preston. 1993. Adsorption of viruses to sand modified by in situ precipitation of metallic salts. Wien. Mitt. Wien 12:25–29.

Foppen, J.W.A., S. Okletey, and J.F. Schijven. 2006. Effect of geothite coating and humic acid on the transport of bacteriophage PRD1 in columns of saturated sand. J. Contam. Hydrol. (in press).

Gerba, C.P. 1984. Applied and theoretical aspects of virus adsorption to surfaces. Adv. Appl. Microbiol. 30:133–168.

Gerritson, J., and S.W. Bradley. 1987. Electrophoretic mobility of natural particles and cultured organisms in freshwaters. Limnol. Oceanogr. 32:1049–1058.

Havelaar, A.H. 1993. Bacteriophages as models of human enteric viruses in the environment. ASM News 59:614–619.

Havelaar, A.H., K. Furuse, and W.M. Hogeboom. 1986. Bacteriophages and indicator bacteria in human and animal feces. J. Appl. Bacteriol. 60:255–262.

Jin, Y., and M. Flury. 2002. Fate and transport of viruses in porous media. Adv. Agron. 77:39–102.

Jin, Y., M.V. Yates, S.S. Thompson, and W.A. Jury. 1997. Sorption of viruses during flow through saturated sand columns. Environ. Sci. Technol. 31:548–555.

Jin, Y., Y. Chu, and Y. Li. 2000. Virus removal and transport in saturated and unsaturated sand columns. J. Contam. Hydrol. 43:111–128.

Johnson, W.P., and B.E. Logan. 1996. Enhanced transport of bacteria in porous media by sediment-phase and aqueous-phase natural organic matter. Water Res. 30:923–931.

Kellogg, R.L., C.H. Lander, D.C. Moffitt, and N. Gollehon. 2000. Manure nutrients relative to the capacity of cropland and pastureland to assimilate nutrients-spatial and temporal trends for the United States. GSA Publication number nsp00–0579. USDA NRCS-ERS, Riverside, CA.

Kinoshita, T., R.C. Bales, K.M. Maguire, and C.P. Greba. 1993. Effect of pH on bacteriophage transport through sandy soils. J. Contam. Hydrol. 14:55–70.

Lukasik, J., Y.F. Cheng, F. Lu, M. Tamplin, and S.R. Farrah. 1999. Removal of microorganisms from water by columns containing sand coated with ferric and aluminum hydroxides. Water Res. 33:769–777.

McCaulou, D.R., R.C. Bales, and R.G. Arnold. 1995. Effect of temperature-controlled motility on transport of bacteria and microspheres through saturated sediment. Water Resour. Res. 31:271–280.

McDowell–Boyer, L.M., J.R. Hunt, and N. Sitar. 1986. Particle transport through porous media. Water Resour. Res. 22:1901–1921.

Pieper, A.P., J.N. Ryan, R.W. Harvey, G.L. Amy, T.H. Illangasekare, and D.W. Metge. 1997. Transport and recovery of bacteriophage PRD1 in a sand and gravel aquifer: Effect of sewage-derived organic matter. Environ. Sci. Technol. 31:1163–1170.

Powelson, D.K., and A.L. Mills. 2001. Transport of Escherichia coli in sand columns with constant and changing water contents. J. Environ. Qual. 30:238–245.

Powelson, D.K., J.R. Simpson, and C.P. Gerba. 1991. Effect of organic matter on virus transport in unsaturated flow. Appl. Environ. Microbiol. 57:2192–2196.

Redman, J.A., S.B. Grant, T.M. Olson, M.E. Hardy, and M.K. Estes. 1997. Filtration of recombinant Norwalk virus particles and bacteriophage MS2 in quartz sand: Importance of electrostatic interactions. Environ. Sci. Technol. 31:3378–3383.

Reynolds, K.A. 2001. Agricultural wastes on groundwater quality: The microbial impact. Water Conditioning and Purification. 43:1.

Ryan, J.N., R.W. Harvey, D. Metge, M. Elimelech, T. Navigato, and A.P. Pieper. 2002. Field and laboratory investigations of inactivation of viruses (PRD1 and MS2) attached to iron oxide-coated quartz sand. Environ. Sci. Technol. 36(11):2403–2413.

Sagripanti, J.L., L.B. Routson, and C.D. Lytle. 1993. Virus inactivation by copper or iron ions alone and in the presence of peroxide. Appl. Environ. Microbiol. 59:4374–4376.

Schijven, J.K., and S.M. Hassanizadeh. 2000. Removal of viruses by soil passage: Overview of modeling, processes, and parameters. Crit. Rev. Environ. Sci. Technol. 30:49–127.

Schijven, J.F., W. Hoogenboezem, S.M. Hassanizadeh, and J.H. Peters. 1999. Modeling removal of bacteriophage MS2 and PRD1 by dune recharge at Castricmn, Netherlands. Water Resour. Res. 35:1101–1111.

Sharma, M.M., Y.I. Chang, and T.F. Yen. 1985. Reversible and irreversible surface charge modification of bacteria for facilitating transport through porous media. Colloids Surf. 16:193–206.

Simunek, J., K. Huang, M. Sejna, and M.Th. van Genuchten. 1998. The HYDRUS-1D software package for simulating the one-dimensional movement of water, heat, and multiple solutes in variably-saturated media-Version 2.0. IGWMC- TPS- 70. International Ground Water Modeling Center, Colorado School of Mines, Golden, Colorado.

USEPA. 2001. Manual of methods for virology. USEPA Rep. 600/4–84/013 (N16). U.S. Gov. Print. Office, Washington, D.C., USA.

Van Duin, J. 1988. The single-stranded RNA bacteriophages. p. 117–167. *In* R. Calendar (ed.) The Bactriophages. Vol. 1. Plenum, New York.

You, Y., G.F. Vance, D.L. Sparks, J. Zhuang, and Y. Jin. 2003. Sorption of MS2 bacteriophage to layered double hydroxides. J. Environ. Qual. 32:2046–2053.

Zerda, K.S. 1982. Adsorption of viruses to charge-modified silica. Ph.D. diss. Baylor College of Medicine, Houston, TX.

Zhuang, J., and Y. Jin. 2003a. Virus retention and transport through Al-oxide coated sand columns: Effects of ionic strength and composition. J. Contam. Hydrol. 60:193–209.

Zhuang, J., and Y. Jin. 2003b. Virus retention and transport as influenced by different forms of soil organic matter. J. Environ. Qual. 32:816–823.